Effects of Different Types of Zeolites on the Degradation Kinetics of Malathion Pesticide in Water

Elly Tety Osewe[1*], Victor Shikuku[2], Cristiane A. Pereira[3], Stephen O. Otieno[4] and Audrey Okoyo[4]

[1]*Kinyanjui Technical Training Institute, Nairobi, Kenya.*
[2]*Kaimosi Friends University College, Kaimosi, Kenya.*
[3]*Federal University of Sao Carlos, Sao Carlos, Brazil.*
[4]*Maseno University, Kisumu, Kenya.*

Authors' contributions

This work was carried out in collaboration among all authors. Authors ETO, CAP, SOO and AO designed the study, performed the statistical analysis, wrote the protocol, and wrote the first draft of the manuscript. Author VS proof read the manuscript. All authors read and approved the final manuscript.

Original Research Article

ABSTRACT

The study examined the effects of selected types of zeolites as an environmentally benign and friendly way to degrade, S-1, 2-bis (ethoxycarbonyl) ethyl O, O-dimethylphosphorodithioate (malathion), used as a model pesticide, from river water. The effect of the size of zeolite channels and dimensionality (such as 1D, 2D, and 3D), Si/Al ratio, and operating pH were studied to find a suitable type of zeolite and conditions to optimize the pesticide degradation. Mordenite (MOR (1D): Si/Al=6.83, and Si/Al=10.72), ferrierite (FER (2D): Si/Al=10.71), ZSM-5 (MFI (3D): Si/Al=6.83 and Si/Al=10.72) and USY (FAU (3D): Si/Al=2.77) zeolites were individually mixed with a water sample collected from Monjolinho River in São Carlos (SP), Brazil and the degradation trend studied. The results showed that all the zeolites accelerated the degradation of malathion. Nevertheless, lower zeolite Si/Al ratio and larger 3D channels or cavities had a positive influence on the degradation rate. The FAU zeolite presented the stronger degradation of the malathion with a half-life of 16.5 followed by ZSM-5 with 24.8, ferrierite with 29.7, and finally mordenite with 30.3 hours.

_____

*Corresponding author: E-mail: tettyosewe@gmail.com;

1. INTRODUCTION

Presently, hundreds of pesticides of varied chemical structures are in use worldwide in the agricultural sector. Unfortunately, most of these compounds migrate from their point of application and enter the aquatic environment via various transport mechanisms such as soil percolation, natural air convection, or runoff among others [1]. Pesticides-polluted waters are also reported to induce ecotoxicological effects on non-target species including humans [2]. Organophosphorus compounds (OPPs), such as S-1, 2-bis (ethoxycarbonyl) ethyl O, O-dimethylphosphorodithioate (malathion), are among the most potent class of insecticides. Malathion, which is being applied as a substitute to dichloro-diphenyl-trichloroethane (DDT), has been repeatedly detected and reported as a persistent contaminant of surface waters in many regions of the world [1,3]. Several studies associate exposure to malathion with mitochondrial dysfunction, endocrine disruption, disruption of male reproductive systems and spermatogenesis in animals, and testicular toxicity, among other disorders [4-8]. Chemically, malathion degrades into its more toxic metabolite malaoxon, which bioaccumulates in living organisms [9].

Several techniques have been reported for the removal of malathion from water. Ishag et al. [10] reported a comparative study on photolysis and photocatalytic degradation of malathion. Though photolysis and photocatalytic degradation sufficiently mineralize malathion, several biologically toxic transformation products such as malaoxon, diethyl maleate, diethyl fumarate, hydroxy butanedioic acid diethylester, among others were detected in the treated effluent. Kanan et al. [11] also reported photodegradation kinetics of malathion by silver exchanged zeolite A. Despite these studies, adsorption is still the widely used technique for the removal of organic contaminants from water due to its simplicity, efficiency, and techno-economic advantages [12]. Several studies have evaluated possible alternative adsorbents such as eggshells, fly ash, zeolites, and clays for malathion removal from water [13-17]. Of particular interest, is the use of zeolites for malathion degradation or sequestration because the structure, properties, and chemistry of zeolite interaction with organic molecules such as pesticides are very specific, arguably complex, and not well understood.

Zeolites are crystalline alumino-silicates composed of three-dimensional networks made by primary building units(PBU), namely, the SiO_4 and AlO_4 tetrahedra, generally referred to as TO_4 tetrahedra [18]. Different zeolite types are identified by the sizes and dimensionalities of their channels and cavities. The sizes of the channels and cavities relative to the kinetic diameters of the pollutant molecules determine whether the molecules are adsorbed within the cavities or on the zeolite surfaces [11,19]. Both the external and internal zeolite surfaces, act as adsorption and reaction sites. It is reported that the selectivity and activity towards organic molecules degradation or sequestration in the environment also depend on the identity of exchangeable cations and can further be tuned by chemical modification [11,20]. Furthermore, due to their varied physical, chemical, and structural properties, zeolites display varied efficacies for each of their numerous applications. The sodium-exchanged Faujasite X (NaX) zeolite (Si/Al<2.5) was reported to be more effective in the degradation and adsorption of Malathion and its residues than Faujasite Y (NaY) zeolite (Si>2.5), and the degradation products were dependent on the type of the zeolite used. The observed variance in performance of the two FAU zeolites was attributed to the zeolites' Si/Al ratios since the zeolites had comparable pore diameters [16]. Both the NaX and NaY zeolites significantly enhanced the malathion degradation kinetics, corroborating previous findings [11]. In a separate study, appreciable changes in unit cell parameters, of the Faujasite Y zeolite following adsorption of the different solutes (sulfonamides) were reported [19]. Similar findings of variation in structural modifications were observed for different zeolites (X and Y) treated with the same malathion adsorbate [16]. These findings underscore the need for a concise comparative investigation of the underlying driving factors of zeolite-catalyzed degradation reactions in pursuit of a selected zeolite with favorable kinetics and adsorption potential for malathion degradation.

In this work, six zeolites samples of varied micropore structural dimensions and Si/Al ratios, viz. mordenite (MOR: Si/Al=6.83 and Si/Al=10.72), ferrierite (FER: Si/Al=10.71), ZSM-5 (MFI: Si/Al=6.83 and Si/Al=10.72) and USY (FAU: Si/Al=2.77), were utilized for the abstraction of malathion from water under laboratory conditions. The effects of the Si/Al

ratio, channel and cavity dimensionality of the zeolites, pH of the suspension besides the time-dependence kinetics, and adsorption equilibrium behavior, modeled using the Langmuir and Freundlich isotherms models, are discussed.
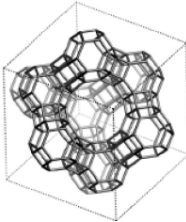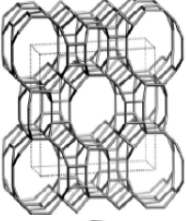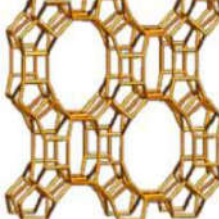
2. MATERIALS AND METHODS

2.1 Reagents and Materials

Malathion *Trace*CERT® standard was purchased from Sigma-Aldrich (99.5% purity). A stock malathion solution (0.5 mg L^{-1}) was prepared with acetone. Other chemicals used, namely, anhydrous n-hexane 95% (Sigma-Aldrich), dichloromethane ACS (Sigma-Aldrich), Acetone ACS (Quemis) (ACS, anhydrous Na_2SO_4 and NaCl (both 99% pure). To approximate the aquatic environment, water collected from Monjolinho River in São Carlos (SP) Brazil

(Class II CONAMA/2005, BRASIL) and spiked with a definite amount of the malathion, was used in the tests of abstraction of the pesticide. The microbial and chemical constituents of the river water, except the presence of malathion, were not determined. No malathion residues were detected in the water samples. Regarding the solid materials, commercial zeolite mordenite MOR CBV-21 (Si/Al=6.83 and Si/Al=10.72) ferrierite FER CP914C (Si/Al=10.71) were purchased from Zeolyst while both ZSM-5 samples (SN27: Si/Al=12.75 and SN-55: Si/Al=23.59) were bought from Alsi-Penta. The applied USY sample (Si/Al=2.77) was donated by the Laboratory of Catalysis of UFSCar/Brazil. The crystalline structure, the dimensionality of the pore structure, pore sizes, Si/Al ratios of the selected zeolites used in the present study are shown in Table 1.

Table 1. Zeolite types and their dimensionality details

Zeolite	Structure	Dimensionality	Pore Dimensions	Si/Al
Faujasite		3D	7.4 (window)	2.8
ZSM-5$_{12}$		3D	5.3 x 5.6	12.8,
ZSM-5$_{23}$		3D	5.3 x 5.6	23.6
Ferrierite		2D	4.3 x 5.5	10.7
Mordenite$_6$		1D	2.9 x 5.7	6.8,
Mordenite$_{10}$		1D	2.9 x 5.7	10.7

Adapted from Structure Commission of the International Zeolite Association (IZA-SC)

2.2 Zeolites Preparation

For the ionic exchange step, 0.1 L of a NaNO$_3$ solution (0.5 mol L^{-1}) was heated on a hot plate till 80°C. After achieving this temperature, 2 g of each zeolite sample (FER, MOR, USY, and ZSM-5) were added remaining under magnetic stirring at 120 rpm for 60 min. The zeolite separation from the suspension was achieved by centrifugation at 3000 rpm for 3.0 min. The solid was thrice-washed using distilled water, then dried in a hot air oven (model 315SE). To purge residual nitrate ions, the dried zeolites were subjected to calcination, following a two-stage procedure. Firstly, the samples were heated from room temperature to 500°C (heating rate = 5°C min^{-1}) in Nitrogen (flow rate 100 mL min^{-1}). Secondly, when the temperature reached 500°C, the N$_2$ flow was replaced by synthetic air (flow rate 100 mL min^{-1}) and kept at this temperature for 4 h.

2.3 Kinetic Studies

Here, 14 set-ups of three replicates were used. Each one runs at 27°C using 100 mL of a solution of 10 mg L^{-1} of malathion in water, containing 1.0 g of each type of pre-treated zeolite. For each replicate, the operational pH of the solutions was measured. At pre-determined time intervals (30 min, 60 min, 90 min, 24 h, 48 h, 60 h, and 72 h), 2 mL aliquots were obtained from the reaction vessels for residual malathion analysis by GC-MS as described by Ogunah et al. [16]. Noteworthy, the malathion recovery ranged from 80.3% to 125.9% (0.1 or 1.0 mg kg^{-1} spiking level), and the linear range of detection was from 0.1 to 8.

Typical GC profiles of the malathion for a standard solution indicated that the malathion and its metabolites (malathion mono (MCA) and dicarboxylic (DCA) acid) were well-separated by the column and the procedure applied.

The amount adsorbed at time *t* was obtained by the equation:

$$q_t = \frac{(c_o - c_t)}{m}V$$

(1)

To obtain the degradation kinetics parameters, the kinetic data were fitted in the first-order equation below.

$$\ln C_t = -kt + \ln C_o$$

(2)

Where *k* and *t* are the rate constant (h^{-1}) and degradation time in h, respectively. C$_o$ and C$_t$ are the concentrations of the pesticide at t = 0 and at time *t*, respectively.

2.4 Equilibrium Studies

To obtain the equilibrium adsorption isotherms, 0.1 g of each zeolite was separately put, in triplicate vessels, and dispersed into reaction flasks containing 50 mL of various concentrations of malathion (5 to 20 mg L^{-1}) and magnetically stirred at 300 rpm and 27°C. After the equilibrium was reached, residual malathion and their degradation products were quantified. The amount adsorbed (%) was obtained by the relation:

$$\%adsorbed = \frac{c_0 - c_e}{c_0} \times 100$$

(3)

The equilibrium adsorption capacity, q_e, at different adsorbate concentration levels was obtained by the equation:

$$q_e = V\frac{(c_0 - c_e)}{m}$$

(4)

The equilibrium adsorption data were then fitted to the Langmuir [21] and Freundlich [22] isotherms. The linearized versions of the isotherm equations are given by:

Langmuir isotherm: $$\frac{1}{q_e} = \frac{1}{Q_0} + \frac{1}{Q_0 K_L C_e}$$

(5)

Freundlich isotherm: $$\log q_e = \log K_1 + \frac{1}{n}\log C_e$$

(6)

Where q$_e$ is the amount adsorbed at equilibrium, C$_e$ is the residual concentration in solution at equilibrium, Q$_o$ is the maximum adsorption capacity, and K$_L$ and K$_F$ are Langmuir and Freundlich constants, respectively.

2.5 Gas chromatographic Conditions

The detection of malathion was done using a Gas Chromatograph Shimadzu GC-2010 coupled to a Shimadzu QP 2010 Plus mass

spectrometer equipped with a capillary column RXI-1MS with 30 m of length, id 0.25 mm and 0.25μm films. To quantify the removal of pesticide, an analytical curve was introduced in the software of the equipment obtained from the injection of solutions with different concentrations prepared from a stock pattern of a malathion solution. Helium was used as carrier gas at a 16.2 mL min^{-1} flow rate, pressure 89.7 kPa, column flow 1.20 mL min^{-1}, linear velocity 40.7 cm s^{-1}, purge flow 3.0 mL/min, and a split ratio of 10.0.2.0 μL of the sample was injected at 200°C. The oven temperature was kept at 100 °C with a hold time of 0 minutes, and then from 100 °C to 300°C at a rate of 10°C min^{-1} with a hold time of 5 mins. The detector was maintained at 300°C.

3. RESULTS AND DISCUSSION

3.1 Degradation Products of Malathion in Water

The occurrence of malathion in the abstraction, as well as the presence of metabolites of the degradation monitored with the time for a reference test, are displayed in Fig. 1. As can be seen, the concentration of malathion, in the absence of zeolite, dropped sharply within the first 9 h then reaching the equilibrium after 22 h. The major degradation products of malathion detected in the current study were the malathion monocarboxylic acid (MCA) and dicarboxylic acid (DCA). The concentration of degradation products (DCA and MCA) slightly increased up to 20 h and thereafter, the concentration of MCA decreased till the end of the experiment. These findings concur with the reports of Lalah and Wandiga [23], who described the transformation of malathion in water, with the major metabolites being malathion α- and β- mono-carboxylic and malathion dicarboxylic acid and that by Ogunah et al. [16]. Such a trend as witnessed in Fig. 1, is characteristic of a consecutive type of reaction inferring that Malathion breaks down to MCA which eventually gives the DCA [16].

In the experiments of malathion degradation in the presence of zeolites, there was no MCA and DCA degradation product found from the GG-MS analyses, however, though the extracts obtained from the zeolites (MOR, FER, MFI, and FAU) residues verified the presence of MCA and DCA, proving their formation and subsequent adsorption on the zeolites. Malaoxon, which is the most toxic of the possible malathion degradation products was effectively not detected from these experiments. The absence of Malaoxon is a boon to the use of zeolites in support of the environmentally benign nature of this technology.
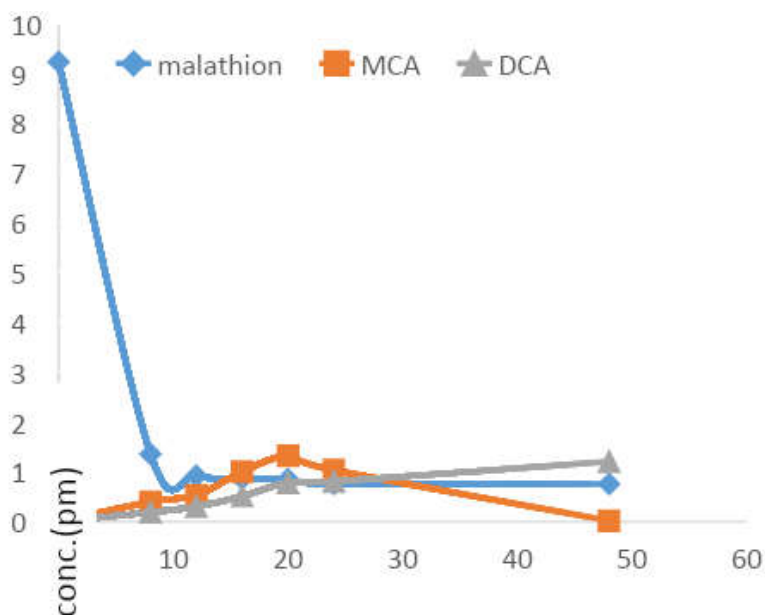

Fig. 1. Distribution of the degradation products from a solution of 10 mg malathion L^{-1} without the presence of any zeolite. MCA is malathion monocarboxylic acid and DCA is malathion dicarboxylic acid

3.2 Degradation of Malathion Pesticide in Water Treated with Different Types of Zeolites

3.2.1 Effects of different zeolites on the resultant reacting pH of the formed suspension

After the zeolites were introduced into the malathion solution, the final operational solution pH was obtained as shown in Fig. 2. As can be observed, the increasing zeolite Si/Al ratio leads to an increase in the resultant pH of the formed suspension. The observed relationship is of practical importance since solution pH is known to enhance or prevent adsorption processes depending on the speciation of the adsorbate molecules and the surface charge of the adsorbent. This charge originates when Al^{3+} is substituted for Si^{4+}, and an extra positive charge is required in the vicinity to counterbalance the O^{2-} [24]. A prominent source of this charge is hydrogen H^+ or H_3O^+ from water, imbuing the Al^{3+} site with acidity which leads to the increase in the solution pH. It is additionally noteworthy, that the degradation of malathion is normally pH-dependent [24].

To monitor the effects of different zeolites on the rates of removal of malathion from the river water, the residual amounts obtained with time were plotted in Table 2. From Table 2, it can be verified that malathion concentration decreases with time in all the experiments. Additionally, a sharp decrease in the concentration of malathion within 8 h was observed whereby mordenite had

88.4%, ferrierite 90.1%, ZSM-5 90.4%, and finally faujasite 90.9%. After 48 h, malathion concentration was below the instrumental detection limit in the analyzed treated solutions for the faujasite, ferrierite, and ZSM-5 treatments. It has been reported that malathion is more susceptible to basic degradation conditions and significant chemical breakdown would therefore be anticipated. However, at 72 h low concentration of malathion was still detectable in the mordenite (Si/Al = 10.7) treatment. This is expected because malathion is stabilized in an acidic medium hence leading to the observed slow degradation (Table 2). It is important to note that aquatic systems are generally buffered and as a result, the overall acidity or basicity of a natural system is not easily affected [25].

Fig. 3 illustrates the trends of the concentration of malathion remaining in the solution as a function of the time after treatment with the zeolites specified in Table 2. Dissipation in river water without zeolite was 89% in the initial 3 h, after which the degradation rate dropped and almost became constant at around 7h. This relatively slower trend is consistent with malathion's reported slow degradation in water at pH < 8.0 [26], for the pH of the river water, was ca. 6.6. Nevertheless, the initial relatively rapid degradation could be attributed to the transformation of malathion to its products which are majorly acids, and as such the pH tends to fall to below 6.6 and would continue dropping as the transformation proceeded, eventually the rate slows down as the amount of malathion remaining decreases [16].
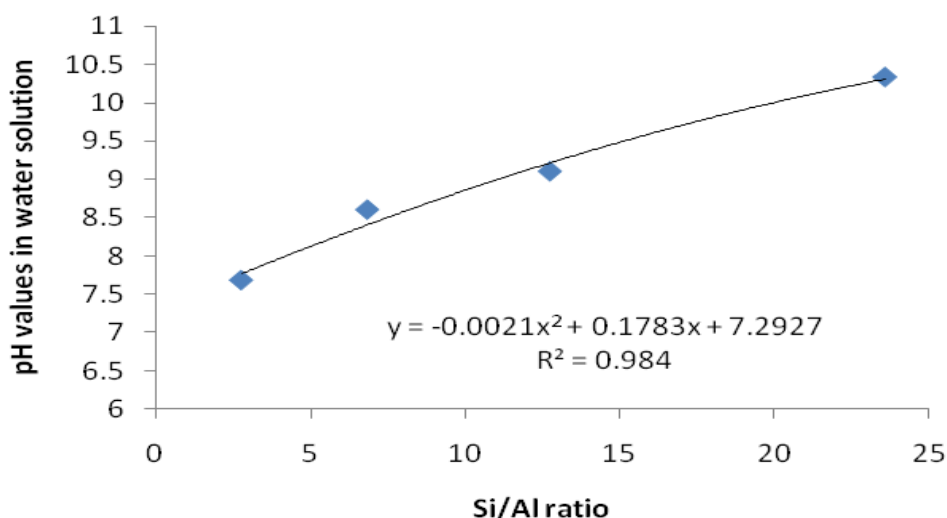

The chart shows pH values in water solution on the y-axis (6 to 11) versus Si/Al ratio on the x-axis (0 to 25), with the equation $y = -0.0021x^2 + 0.1783x + 7.2927$ and $R^2 = 0.984$.

Fig. 2. Variation of the resultant pH as a function of the Si/Al ratio of the zeolite

Table 2. Residual malathion mean concentration with time in water treated with six different types of Na-exchanged zeolites at 27°C (n.d: not detected)

| Zeolite type	Si/Al	pH	Residual concentration (mg/L) at different times (h)						
			8h	12h	16h	20h	24h	48h	72h
Faujasite-	2.8 ±0.05	7.68 ± 0.05	0.912 ± 0.044	0.854 ± 0.027	0.663 ± 0.036	0.565 ± 0.014	0.484 ± 0.033	n.d	n.d
Mordenite$_6$	6.8 ± 0.05	8.6 ± 0.05	1.210 ± 0.041	1.190 ± 0.024	0.988 ± 0.033	0.907 ± 0.012	0.877 ± 0.053	0.679 ± 0.044	n.d
Mordenite$_{10}$	10.7 ± 0.05	4.1 ± 0.05	1.163 ± 0.027	0.986 ± 0.018	0.942 ± 0.045	0.875 ± 0.011	0.807 ± 0.043	0.743 ± 0.046	0.565 ± 0.014
ZSM-5$_{12}$	12.8 ± 0.05	9.1 ± 0.05	0.996 ± 0.036	0.928 ± 0.055	0.872 ± 0.046	0.743 ± 0.046	0.679 ± 0.044	n.d	n.d
ZSM-5$_{23}$	23.6 ± 0.05	10.33 ± 0.05	0.991 ± 0.034	0.847 ± 0.025	0.728 ± 0. 032	0.699 ± 0.027	0.614 ± 0.04	n.d	n.d
Ferrierite-	10.7 ± 0.05	5.3 ± 0.05	0.987 ± 0.026	0.907 ± 0.022	0.853 ± 0.042	0.760 ± 0.043	0.677 ± 0.046	n.d	n.d
Control	0.0 ± 0.05	6.6 ± 0.05	1.036 ± 0.030	0.923 ± 0.044	0.892 ± 0.034	0.869 ± 0.054	0.853 ± 0.042	0.760 ± 0.043	0.679 ± 0.044
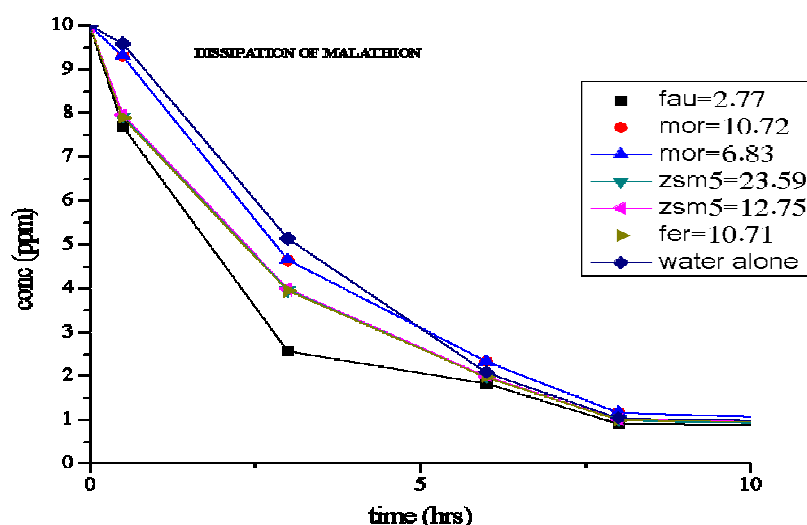
Fig. 3. Concentration of malathion as a function of the time in water treated with the zeolites. The initial malathion concentration was 10 mg L^{-1}

Upon the addition of the zeolites, the dissipation rate became faster relative to the control experiments. This increased dissipation was attributed to a combination of two factors: elevated solution pH effect and enhanced catalytic action that lead to faster degradation and/or adsorption of the zeolites. Since the solution pH increased when zeolite was added (see Fig. 2), faster initial degradation was expected due to the high pH effect which generally enhances the degradation of malathion [26]. Notably, the degradation rate in faujasite was faster than the rest of the treatments followed by ferrierite and MFI, and finally MOR (Fig. 3). This is explained by the fact that in alkaline conditions, the higher silica zeolites show decreased base stability as compared to the lowest silica zeolite (faujasite). This enhanced degradation means that faujasite catalysis is highly favored in such conditions. Besides, the generation of alkaline media of the zeolite suspensions, the zeolites could also possess catalytic and adsorption properties [24]. Thus, these factors combined contributed to the hastened malathion dissipation rate.

3.3 Degradation Kinetics of Malathion Pesticide

The degradation rate constants and half-lives of the malathion were calculated from the data in Table 2 using the first-order kinetics model (equation 2), and the values are listed in Table 3. From Table 3, malathion degradation in water was increased by the introduction of all zeolites.

The findings show that FAU zeolite exhibited more effect on the degradation of malathion than the other zeolites used. A similar phenomenon was reported by Ogunah et al. [16] upon comparing X and Y type zeolites. The applied zeolites showed different impacts on malathion degradation in terms of Si/Al. Surprisingly, when two MFI zeolite samples (ZSM-5: Si/Al = 12.8 and 23.6) and two other mordenite zeolite samples (MOR: Si/Al = 6.8 and 10.7) with each series differing only in its Si/Al ratio are analyzed, the effect of that difference was not pronounced. Specifically, mordenite (Si/Al=6.8) exhibited stronger acceleration on the degradation of malathion than mordenite (Si/Al=10.7), as the former presented a higher pH and consequently higher rate constant. On the other hand, ferrierite (Si/Al=10.7) exhibited a slightly stronger mineralization of malathion with a half-life of 29.7 h when compared to 32.5 h for mordenite with the same Si/Al ratio.

However, the pointed differences, Fig. 4 shows that irrespective of the zeolite structure, for Si/Al ratios higher than 5, it can be observed a clear tendency of an increase of the rate of malathion degradation with the increase of the Si/Al ratio.

Micropores structure dimensionality in zeolites (D), whether 1D, 2D, or 3D (Table 1), also affects the rate of molecule removal in the treatment media [24]. Fig. 5 shows the relationship between dimensionality and the half-life of malathion degradation in the studied aqueous malathion solution with R^2 approx. 0.7.

Table 3. Half-live and degradation rate constant of malathion in river water

Zeolite type	Parameters					
	D	pH	Si/Al	$k(h^{-1})$	R^2	$t_{1/2}(h)$
Faujasite	3D	7.7	2.8	0.0420	0.979	16.5
Mordenite$_{10}$	1D	4.1	10.7	0.0213	0.955	32.5
Mordenite$_6$	1D	8.6	6.8	0.0229	0.926	30.3
ZSM-5$_{23}$	3D	10.3	23.6	0.0279	0.964	24.8
ZSM-5$_{12}$	3D	9.1	12.8	0.0247	0.972	28.1
Ferrierite	2D	5.3	10.7	0.0233	0.986	29.7
NONE-control	-	6.6	NONE	0.0140	0.874	49.5

(k: degradation rate constant; R^2, coefficient of determination; $t_{1/2}$, half-life period; D: Dimensionality)
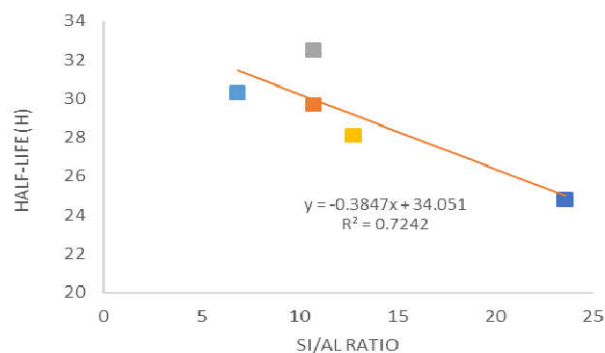

Fig. 4. Relationship between the half-lives of the malathion dissipation and the Si/Al ratio for Si/Al ratios higher than 5
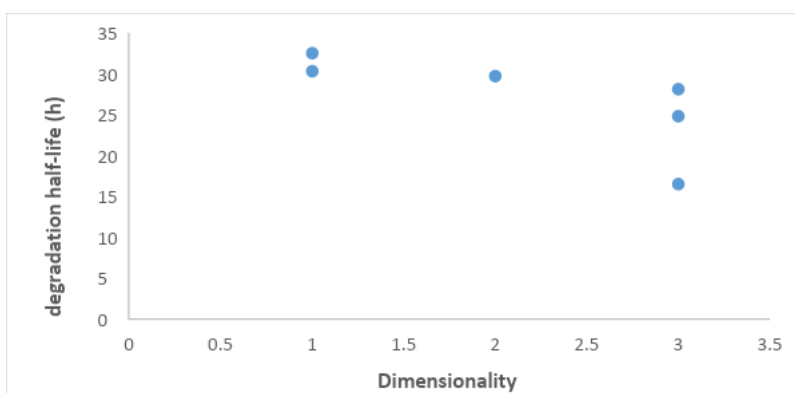

Fig. 5. Changes in Malathion dissipation half-life with zeolite dimensionality

Table 4. Langmuir and freundlich parameters for malathion adsorption by zeolites from aqueous solution at 27°C

Zeolites	Langmuir Isotherm			Freundlich Isotherm		
	q_{max} (mg/g)	K_L (L/mol)	R^2	n	K_F	R^2
Ferrierite (Si/Al=10.7)	2.079	0.921	0.914	1.934	8.723	0.814
Mordenite (Si/Al=10.7)	0.722	1.138	0.847	1.314	8.551	0.727
Mordenite (Si/Al=6.8)	0.722	1.138	0.847	1.314	8.551	0.727
MFI (Si/Al=23.6)	2.070	0.886	0.911	2.016	8.472	0.800
MFI (Si/Al=12.8)	2.012	1.835	0.912	1.901	8.750	0.810
USY(Si/Al=2.8)	3.300	1.000	0.952	7.299	8.723	0.944

According to Fig. 5, the 3D zeolites (FAU and ZSM-5) clearly show relatively higher malathion degradation with half-lives between 6 to 28 h. The 2D ferrierite has an intermediate half-life of ca. 29 h, while the 1D mordenite presents $t_{\frac{1}{2}}$ between 30 and 32.5 h. According to [24], the channel dimensions of the zeolites strongly affect molecule removal. Besides size exclusion effects, molecules that do fit in the zeolitic channels, smaller molecules are removed more effectively when they fitted tightly within the channels, because of larger van der Waals interactions. However, due to the large size of the malathion molecule (10.8-11.9 Å), the molecules cannot penetrate the zeolite channels. Therefore, catalytic degradation and adsorption of malathion by the zeolites occur on their surfaces.

3.4 Adsorption Studies

The adsorption equilibrium data were modeled using linearized Freundlich and Langmuir isotherms and the calculated parameters are presented in Table 4. The Langmuir isotherm better described the equilibrium data as shown by the relatively higher coefficient of determination (R^2) values in comparison to the Freundlich isotherm. Close adherence to the Langmuir isotherm implies that the maximum adsorption occurs when a saturated monolayer of malathion molecules was present on the adsorbent surface, the energy of adsorption was constant and there was no migration of pesticide molecules in the surface plane [27]. Higher K_L values, as in MFI zeolite (Si/Al=12.8), are associated with strong bonding of malathion to the zeolite [25]. The similarity in the adsorption capacities of the 1D mordenite zeolites despite the dissimilarity of their Si/Al ratio implies that there was no direct relationship between the Si/Al ratios and the maximum adsorption capacities predicted from the isotherm models. A similar observation was made between the 3D MFI (Si/Al=12.8) and the MFI (Si/Al=23.6) zeolites. These results suggest that the adsorption capacity is mostly controlled by dimensionality and less by Si/Al ratios. As such, the adsorption capacity increased with the dimensionality in the order 1D<2D<3D.

4. CONCLUSION

The present study shows that the degradation kinetics of malathion in the river water was impacted by the treatment with mordenite (MOR), ferrierite (FER), ZSM-5 (MFI), and USY

(FAU) zeolites. All zeolites impeded the generation of more toxic products such as Malaoxon. The Faujasite and ZSM-5 (MFI) were more effective when compared to mordenite and ferrierite zeolites. USY (FAU) zeolite exhibited a stronger enhancing impact on the degradation of malathion. Among the characteristics of zeolites used, the dimensionality of the zeolitic pores was more pronounced in determining the removal of malathion. Even though the Si/Al ratio had a profound influence on the solution pH, there is a weak relationship between the Si/Al ratios and the maximum adsorption capacities, residual pesticide amounts, and the half-life of degradation reactions. Future works should examine the performance of the zeolites on a pilot scale including recyclability and cost-analysis, before possible utilization on large-scale systems.

DISCLAIMER

ACKNOWLEDGEMENTS

COMPETING INTERESTS

Authors have declared that no competing interests exist.

REFERENCES

1. Gao JL. The Occurrence and Spatial Distribution of Organophosphorous Pesticides in Chinese Surface Water. bull Environ Contam Toxicol. 2009;82(2):223-229.

2. Howard PH. Handbook of environmental fate and exposure data for organic Chemicals vol 3:pesticides. Chelsea: Lewis Publishers; 1991.

3. Sankararamakrishnan N, Sharma AK, Sanghi R. Organochlorine and organophosphorous pesticide residues in ground water and surface waters of Kanpur, Uttar Pradesh, India. Environ. Inter. 2005;31(1):113-120.

4. Geng X, Shao H, Zhang Z, Ng JC, Peng C. Malathion-induced testicular toxicity is associated with spermatogenic apoptosis and alterations in testicular enzymes and hormone levels in male Wistar rats. Environ. Toxicol. Pharmacol. 2015;39(2):659-667.

5. Karami-Mohajeri S, Hadian MR, Fouladdel S, Azizi E, Ghahramani MH, Hosseini R, Abdollahi M. Mechanisms of muscular electrophysiological and mitochondrial dysfunction following exposure to malathion, an organophosphorus pesticide. Hum. Exp. Toxicol. 2014;33:251–263.

6. Mnif W, Hassine AI, Bouaziz A, Bartegi A, Thomas O, Roig B. Effect of endocrine disruptor pesticides: a review. Int. J. Environ. Res. Public Health. 2011;8:2265–2303.

7. Jira D, Janousek S, Pikula J, Vitula F, Kejlova K. Toxicity hazard of organophosphate insecticide malathion identified by in vitro methods. Neuro Endocrinol. Lett. 2012;33(Suppl. 3):53–59.

8. Choudhary N, Goyal R, Joshi SC. Effect of malathion on reproductive system of male rats. J. Environ. Biol. 2008;29:259–262.

9. Budischak SA, Belden LK, William AH. Relative toxicity of malathion to trematode-infected and noninfected Rana palustris tadpoles. Arch. Environ. Contam. Toxicol. 2009;56(1):123-128.

10. Ishag AESA, Abdelbagi AO, Hammad AMA, et al. Photodegradation of chlorpyrifos, malathion, and dimethoate by sunlight in the Sudan. Environ Earth Sci. 2019;78:89.
Available:https://doi.org/10.1007/s12665-019-8064-z

11. Kanan SM, Kanan C, Patterson H. Photophysical properties of Ag(I)-exchanged zeolite A and the photoassisted degradation of malathion. J. Physical Chem. B. 2001;105(31):7508–7516.

DOI: 10.1021/jp010184j

12. Ng'eno E, Shikuku VO, Orata F, Lilechi DB, Kimosop S. Caffeine and ciprofloxacin adsorption from water onto clinoptilolite: Linear isotherms, kinetics, thermodynamics, and mechanistic studies. S. Afr. J. Chem. 2019;72:136-142.

13. Gupta VK, Jain CK, Ali I, Chandra S, Agarwal S. Removal of lindane and malathion from wastewater using bagasse fly ash—a sugar industry waste. Water Res. 2002;36(10):2483-2490.

14. Elwakeel KZ, Yousif AM. Adsorption of malathion on thermally treated egg shell material. Water Sci. Technol. 2010;61(4):1035-41.

15. Ahmed MD, Asem AA, Rashad AH, Rama TR. Comparative study on the adsorption of malathion pesticide by different adsorbents from aqueous solution, Desalination Water Treatment. 2012;47:1-3,300-309.

16. Ogunah JA, Kowenje CO, Osewe ET, Lalah JO, Jaoko DA, Koigi RN. Effects of zeolites X and Y on the degradation of malathion in water. Sci. J. Chem. 2013;1(1):7-13.

17. Shikha S, Adya J, Kautily RT, Neeraj K, Radha T. Synthesis and characterization of zeolite linde w and its application as adsorbent for Malathion. Inter. J. Current Res. 2018;10(11):75472-75476.

18. Margeta K, Zabukovec N, Siljeg M, Farkas A. Natural zeolites in water treatment – How effective is their use. Water Treatment; 2013.
DOI: 10.5772/50738

19. Braschi I, Blasioli S, Gigli, Lara, Gessa C, Alberto A, Martucci A. Removal of sulfonamide antibiotics from water: Evidence of adsorption into an organophilic zeolite Y by its structural modifications. J. Hazard. Mater. 2010;178:218–225.

20. Kowenje CO, Schulte J, Kanyi CW, DeCoste J, Yang SW, Jones BR. Effects of copper exchange levels on complexation of ammonia in Cu (II)-exchanged X zeolite. S. Afr. J. Chem. 2010;63:6-10.

21. Langmuir I. The adsorption of gases on plane surfaces of glass, mica and platinum. J. Am. Soc. 1918;40:1361-1403.

22. Freundlich HMF. Over the adsorption in solution. J. Phys. Chem. 1906;57:385-470.

23. Lalah JO, Wandiga SO. The effect of boiling on the removal of persistent malathion residues from stored grains. J. stored prod. res. 2002;38(1):1-10.

24. Kowenje CO, Osewe ET. Optimizing zeolitic catalysis for environmental remediation. In In Advanced Catalytic Materials. John Wiley & Sons, Inc. 2015;411-438.

25. Battala G, Yadamari T, Korivi SK, Gurijala RN, Singhal RK. Study on degradation of malathion and phorate in various environmental matrices. Afr. J. Environ. Sci. Technol. 2012;6(5):224-228.

26. Newhart K. Environmental fate of malathion. California Environmental Protection Agency; 2006.

27. Shikuku VO, Donato FF, Kowenje CO, Zanella R, Prestes D. A comparison of Adsorption Equilibrium, Kinetics and Thermodynamics of Aqueous phase Clomazone between Faujasite X and a Natural zeolite from Kenya. S. Afr. J. Chem. 2015;68:245-25.

Peer-review history:
The peer review history for this paper can be accessed here:
http://www.sdiarticle4.com/review-history/69829